All Photons Imaging Through Thick Layered Scattering Materials

Guy Satat, Barmak Heshmat, Ramesh Raskar
Media Lab, Massachusetts Institute of Technology, Cambridge, MA 02139, USA
guysatat@mit.edu

Abstract: We demonstrate a method to image through thick layered scattering materials. The method uses time-resolved measurement and leverages all of the optical signal to computationally invert the scattering.

OCIS codes: (110.0113) Imaging through turbid media, (110.1758) Computational imaging, (290.0290) Scattering.

1. Introduction

Imaging though thick highly scattering media (sample thickness $\gg$ mean free path) can realize broad applications in biomedical and industrial imaging as well as remote sensing. Various modalities to see through scattering usually require locking into a specific part of the optical signal, such as coherent [1], ballistic [2], or acoustically modulated photons [3]. As a result, these methods reject most of the optical signal and operate at lower signal-to-noise ratio (SNR). On the other hand All Photon Imaging (API) [4] revitalizes the conventionally lost portion of the signal, and demonstrates imaging through thick barriers by computationally inverting the scattering.

API is based on time-resolved measurement and uses both early (ballistic and snake) and diffused photons. API is an all-optical, calibration-free framework which enables wide-field imaging through thick, highly scattering turbid media. Since API does not rely on intrinsic properties of the optical signal (for example coherence or polarization), it can scale well to long range sensing. This makes it appealing for biomedical applications such as full organ imaging, as well as remote sensing configurations such as imaging through fog and clouds.

Here, we use Monte Carlo simulations to demonstrate that API can image through thick scattering materials composed of different layers (in-homogeneous in the optical axis). The ability to see through layered materials is important for biomedical applications where the scattering is due to different layers (skin, fat, muscle etc.).

2. API Operating Principle

For clarity, we provide basic details on API, for more details on setup and formulation see [4]. API uses time-resolved measurement to map an unknown two dimensional scene to a three dimensional measurement, such that:

$$m(x,y,t) = \alpha K(x,y,t) * s(x,y) \tag{1}$$

where $m(x,y,t)$ is the time-resolved measurement, $s(x,y)$ is the unknown 2D scene, and $K(x,y,t)$ is the scattering kernel which also performs the mapping from $x-y$ to $x-y-t$. α is a scaling parameter. API works in optical transmission mode, the target plane is defined as $z=0$, and the measurement plane as $z=L$ where L is the total thickness of the material. $K(x,y,t)$ can be considered as the probability to measure a photon at position x,y and time t. This can be used to break the kernel $K(x,y,t)$ with the Bayes rule:

$$K(x,y,t) = f_T(t)W(x,y|t) \tag{2}$$

Here, $f_T(t)$ is the probability to measure a photon at time t independent of its position, and $W(x,y|t)$ is the probability to measure a photon at a specific position given that time. We note that $f_T(t)$ doesn't capture any spatial information, thus it is only a function of the scattering material and not the hidden target. $f_T(t)$ is robustly estimated from the measurement itself by choosing the time series $m(x_0,y_0,t)$ with the strongest signal. This estimation captures time-resolved information about ballistic, snake and diffused photons without making any assumptions. Then, the measurement $m(x,y,t)$ can be normalized by $f_T(t)$ such that: $\tilde{m}(x,y,t) = m(x,y,t)/f_T(t)$.

Next we define the $W(x,y|t)$ term. Given the photons' time of arrival to the sensor t, the spatial distribution follows the law of large numbers and is modeled as a Gaussian distribution (assuming a homogeneous material in the $x-y$

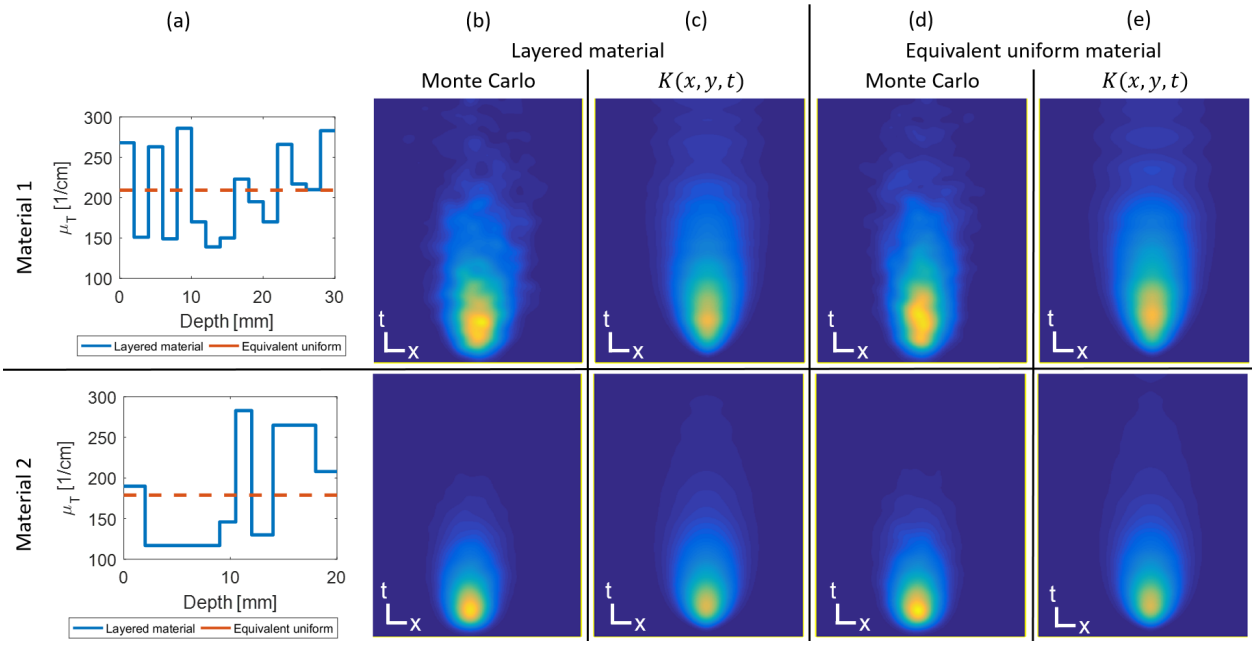

Fig. 1. PSF of layered and equivalent uniform materials and API model estimation. (a) cross section of the extinction coefficient μ_T in different depths. μ_T was sampled from uniform distribution in the range $[100,300]$ cm^{-1}. The material has 15 layers with identical thickness $l_k = 2mm$, and the overall thickness is $L = 30mm$. The equivalent uniform material extinction coefficient (Eq. 5) appears as dashed orange line. (b) Monte Carlo simulation result for a point source through the layered material. 10^7 photons are simulated. The result shows the $x-t$ cross section for $y = 0$. (c) The evaluated model $K(x,y,t)$. (d) Monte Carlo simulation of the equivalent uniform material. (e) Evaluated model $K(x,y,t)$ of the uniform material. Bottom row shows similar results for a material composed of 8 layers with varying thicknesses. We note that columns b-e shows similar features. This indicates the similar behavior of the layered structure and a single layer with averaged extinction coefficient.

axes). The distribution has a time dependent variance. In our experiments we find that a linear time dependent variance is sufficient (this is also similar to the diffusion equation):

$$W(x,y|t) = \exp\left\{-\frac{x^2+y^2}{D(t-t_0)}\right\} \tag{3}$$

here, D captures the diffusive behavior and t_0 captures the material thickness. Both D and t_0 are estimated from the measurement in a calibration-free manner (see [4]).

Finally, with the estimated forward model, the scattering is computationally inverted by solving:

$$s = \arg\min_{\hat{s}} \left\{ \|\mathbf{A}\hat{s} - \tilde{m}\|_2^2 + \lambda \|\hat{s}\|_1 \right\} \tag{4}$$

where $\mathbf{A}$ is a matrix with columns defined by $W(x,y|t)$, and λ is a regularization parameter ($\lambda = 0.0025$ in all presented results). Here we use an l_1 regularizer which is a good prior for the targets we use.

3. API and layered materials

The measurement apparatus of API captures no direct information on the scattering dynamics within the materials (specifically no information about the z coordinate). These dynamics are averaged and encoded in the measurement from the material boundary. It is interesting to note that Eq. 1 assumes a homogeneous material in the $x-y$ coordinates (due to the convolution) but there is no such assumption on the z axis. Thus, API is invariant to variations in the scattering properties along the z axis. To demonstrate this invariant behavior we consider a layered material with K

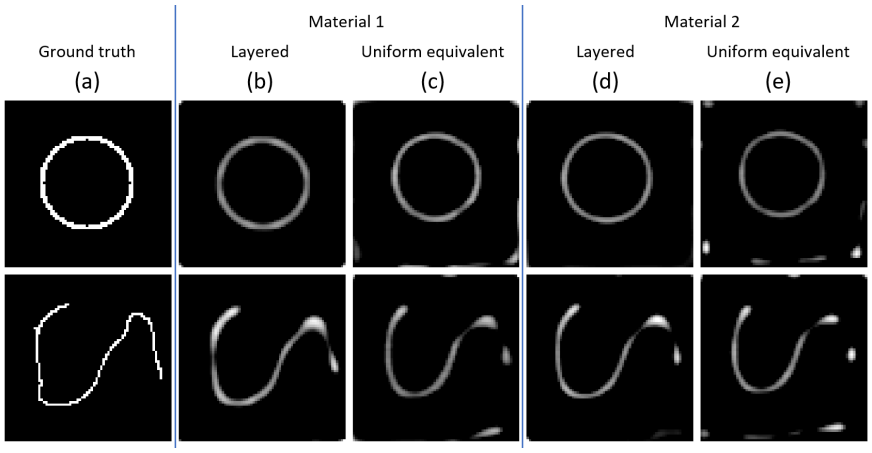

Fig. 2. API successfully recovers targets (rows) hidden behind layered materials. (a) Ground truth. (b) Reconstruction of target hidden behind material 1 (Fig. 1 top – 30 *mm* thick, 15 layers with equal thicknesses). (c) Reconstruction of target behind the uniform equivalent. (d) and (e) Similar for material 2 (Fig. 1 bottom – 20 *mm* thick, 8 layers with varying thicknesses). We note that apart from edge artifacts the reconstruction quality is similar in all cases indicating that API is invariant to variations of the extinction coefficient along the optical axis. We also note that while material 1 and 2 are very different with notable different PSFs (2 vs. 3 *cm* thick, 2× number of layers, uniform and non-uniform layer thicknesses), API is able to reconstruct the targets with comparable quality.

layers with different extinction coefficients μ_{T_k} and different thickness l_k (such that $L = \sum l_k$). Since API is invariant to these individual coefficients there is an equivalent uniform material with an extinction coefficient μ_{T_U} such that:

$$\mu_{T_U} = \sum_{k=1}^{K} \frac{l_k}{L} \mu_{T_k} \tag{5}$$

This model has several limitations, primarily it neglects the effects of changes in index of refraction in the transition between layers. This can be addressed by modeling the index of refraction as a function of the extinction coefficient and adding an appropriate transmission/reflection probability between the layers interfaces.

Fig. 1 demonstrates Monte Carlo simulation results for various layered materials. In these simulations each layer k has a different extinction coefficient μ_{T_k} and thickness l_k. We consider two materials with different extinction coefficients, number of layers and thicknesses as well as the equivalent uniform materials. We demonstrate the simulated point spread function (PSF) for all materials and the estimated PSFs $K(x,y,t)$ based on section 2. Lastly, Fig. 2 demonstrates reconstruction of targets hidden behind these layered materials, and the equivalent uniform materials. All examples demonstrate that API is invariant to changes in the extinction coefficient along the z axis.

4. Conclusions

We use Monte Carlo simulations to demonstrate that API method scales to layered materials with non-homogeneous profile in depth. This is important for potential applications in biomedical imaging. Future work will explore overcoming non-homogeneous materials in the $x-y$ axes as well as operating in optical reflection mode.

References

1. D Huang, E Swanson, C Lin, J Schuman, W Stinson, W Chang, M Hee, T Flotte, K Gregory, C. Puliafito, and Al. Et. Optical coherence tomography. *Science*, 254(5035):1178–1181, 1991.
2. L Wang, P P Ho, C Liu, G Zhang, and R R Alfano. *Science (New York, N.Y.)*, 253(5021):769–71, 1991.
3. X Xu, H Liu, and L V Wang. Time-reversed ultrasonically encoded optical focusing into scattering media. *Nature Photonics*, 5:154–157, 2011.
4. G Satat, B Heshmat, D Raviv, and R Raskar. All Photons Imaging Through Volumetric Scattering. *Scientific Reports*, 6:33946, 2016.